International Journal of Thermophysics, Vol. 22, No. 2, 2001

Measuring Speed of Sound and Thermal Diffusivity in the Diamond-Anvil Cell[1]

E. H. Abramson,[2, 3] J. M. Brown,[4] L. J. Slutsky,[2] and S. Wiryana[2]

Transient grating spectroscopy in the diamond-anvil high-pressure cell permits, in favorable cases, determination of the equation of state and thermal transport properties of fluids at high temperatures and pressures. Measurements of the speed of sound and thermodynamic properties of aqueous Na_2SO_4 to 3.4 GPa at 300°C and the thermal diffusivity of oxygen are reported as examples of the application of this technique.

KEY WORDS: chemical potential; diamond-anvil cell; equation of state; high pressure; oxygen; sodium sulfate; thermal conductivity; thermal diffusivity; transient grating spectroscopy.

1. INTRODUCTION

The thermodynamic properties and transport coefficients of simple fluids at high temperatures and pressurs play an important role in the earth [1] and planetary [2] sciences. These quantities also provide a necessary test of empirical potentials from which the equation of state and other kinetic and thermodynamic properties under experimentally difficult conditions might be deduced. Although there have been extensive studies of the properties of liquids in conventional piston-cylinder high-pressure systems, the thermodynamic properties of liquids and solutions in much of the higher-pressure portion of the pressure–temperature plane accessible in the diamond-anvil cell are not conveniently investigated. Similarly, the experimental study of transport properties at high pressures has proven to be difficult. The thermal

[1] Paper presented at the Fourteenth Symposium on Thermophysical Properties, June 25–30, 2000, Boulder, Colorado, U.S.A.

[2] Department of Chemistry, University of Washington, Seattle, Washington 98195, U.S.A.

[3] To whom correspondence should be addressed. E-mail: evan@geophys.washington.edu

[4] Department of Geophysics, University of Washington, Seattle, Washington 98195, U.S.A.

0195-928X/01/0300-0405$19.50/0

diffusivity of liquid water has been reported only at pressures below 0.8 GPa [3], although water and aqueous mixtures are principal detonation products, and the properties of water at much higher pressures are important in geophysical and geochemical modeling [1]. Measurements for diatomic gases by traditional techniques have not been extended beyond 1.0 GPa [4].

Transient grating spectroscopy [5, 6] permits the determination of both the thermal diffusivity and the speed of sound in the heated, diamond-anvil cell [7, 8]. From the pressure and temperature dependence of the speed of sound, the equation of state of a fluid a can be deduced. Thus, in a solution the pressure dependence of the chemical potential of a solute species can be calculated. Examples are given here from studies of aqueous Na_2SO_4 and fluid oxygen extending to temperatures of 300°C and to pressures of 3.4 and 13 GPa, respectively.

2. SPEED OF SOUND

In the experiments reported here two successive "excitation" pulses, ≈ 80 ps in duration, selected from the output train of a Q-switched, mode-

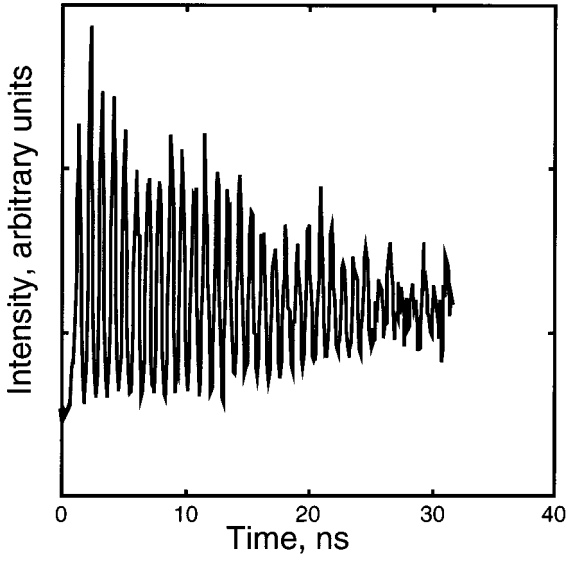

Fig. 1. Scattered intensity as a function of probe delay in $0.5m$ Na_2SO_4 at 89°C and 1.82 GPa. The frequency is 1.0735 GHz, and the wavelength is 3.011 μm, corresponding to an angle of intersection of 20°.

locked, Nd:YAG laser are recombined in the sample at an angle 2θ, but otherwise coincident in space and time. Interference establishes a periodic distribution of intensity. In a sample that absorbs at the wavelength of the laser light, $\lambda_{IR} = 1.064\,\mu$m, a (spatially) periodic variation in the temperature ensues. The associated thermal pressure launches counterpropagating acoustic waves. The acoustic wavelength λ_A, expressed in terms of λ_{IR} and θ, is

$$d = \lambda_A = \frac{\lambda_{IR}}{2 \sin \theta} \tag{1}$$

The impulsively excited acoustic waves induce a temporally and spatially periodic variation in the index of refraction of the sample. A third pulse, selected from the same Q-switched envelope as the excitation pulses, is doubled to 532 nm and delayed by time of flight to generate the probe. Observation of the intensity of the Bragg scattering of the probe by the acoustic grating as a function of probe delay serves to determine the frequency (f_A), and, hence, the speed of sound ($c = \lambda_A f_A$), as well as the attenuation of the acoustic waves.

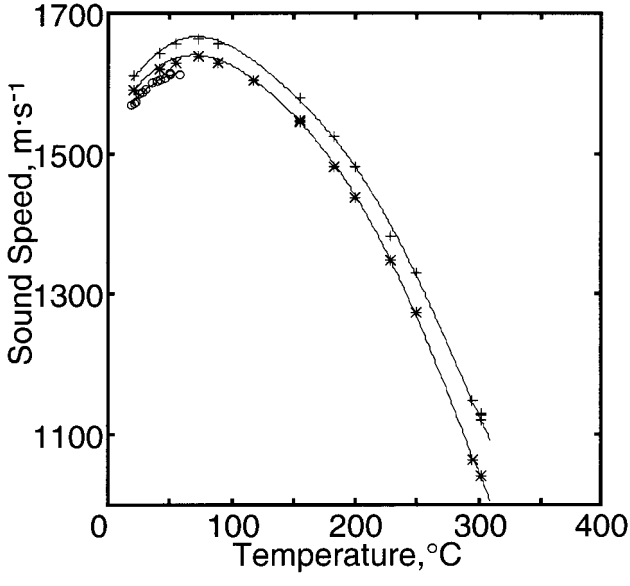

Fig. 2. Speed of sound in $0.5m$ Na_2SO_4 at representative pressures between 0.1 and 27.6 MPa at temperatures between 20 and 300°C. (○) Data at 1 bar; (∗) data at 13.8 MPa; (+) results at 27.6 MPa.

A representative time-domain record for 0.5 molal (m) aqueous Na_2SO_4 at 89°C and 1.82 GPa in an inconel-gasketed diamond-anvil cell is shown in Fig. 1. The apparent decay of the acoustic modulation here stems from purely geometric attenuation as the acoustic disturbance propagates beyond the volume illuminated by the probe (the separation of geometric attenuation from absorption is discussed in Ref. 7), and no dispersion that might be indicative of slow chemical or structural relaxation is observed.

Speeds of sound in aqueous Na_2SO_4 have been measured as functions of temperature, pressure, and composition both in a Merrill–Basset diamond-anvil cell and at pressures below 0.03 GPa in a conventional cell fabricated from Inconel 625 with optical access through sapphire windows. Data at pressures up to 0.03 GPa are displayed in Fig. 2. Results to 3.4 GPa in the diamond-anvil cell are given in Fig. 3 and in Table I.

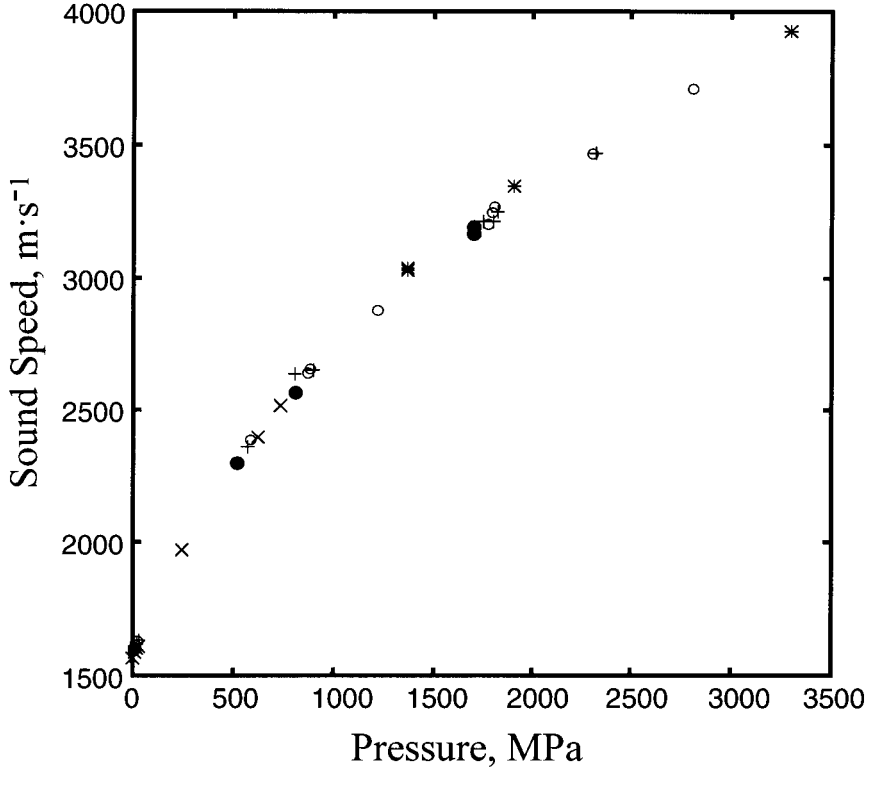

Fig. 3. Speed of sound in 0.5m aqueous Na_2SO_4 as functions of temperature and pressure. Data at 20°C (×); data at 89°C (●); data at 117°C (+); data at 130°C (○); data at 200°C (∗). Pressures in the diamond-anvil cell are measured by ruby fluorescence [9–11].

Table I. Interpolated Speeds of Sound ($m \cdot s^{-1}$) in Aqueous 0.5*m* Na_2SO_4 as a Function of Temperature and Pressure

	T (°C)								
P (MPa)	20.4	40.4	73.7	89.4	117.1	130.0	200.0	250.0	300.0
0.10	1567	1603	1614	1599					
2.4	1571	1606	1618	1604	1578				
4.5	1575	1609	1621	1609	1583	1574		1239	1013
16	1594	1624	1642	1633	1606	1598	1447	1274	1057
27	1612	1641	1661	1656	1629	1620	1481	1321	1123
200	1895	1900	1941	1934	1916	1922	1821		
400	2177	2165	2206	2181	2182	2184	2116		
600	2393	2391	2416	2388	2402	2397	2358		
800	2544	2586	2587	2568	2589	2571	2564		
1200			2869	2871	2893	2866	2902		
1400			3000	3001	3019	2995	3044		
1600			3132	3120	3132	3114	3172		
1800			3207	3229	3234	3225	3289		
2000					3327	3330	3396		
2200					3412	3430	3494		
2800						3702	3747		
3200							3889		
3400							3954		

At temperatures where the density and heat capacity of a fluid or solution are known at, at least, one point on an isotherm, the equation of state at a fixed composition can be determined by recursive integration of

$$\left(\frac{\partial \rho}{\partial P}\right)_T = \frac{1}{c^2} + \frac{T\alpha^2}{c_p} \quad \text{and} \quad \left(\frac{\partial c_p}{\partial P}\right)_T = -T\frac{\partial^2 v_{sp}}{\partial T^2} \tag{2}$$

where ρ is the density, α is the coefficient of thermal expansion, c_p is the specific heat, and v_{sp} is the specific volume. To deduce v_{sp} at higher temperatures, the Gibbs free energy per gram at each composition is expanded about a convenient temperature and pressure in the form,

$$G_{sp} = \sum_{ij} A_{ij} P^i T^j \tag{3}$$

Equation (3) is then appropriately differentiated and the coefficients adjusted to match the P, v_{sp}, T relations and the pressure dependence and temperature dependence of the heat capacity (where known), in addition to the measured speed of sound at high temperatures and pressures. The continuous curves in Fig. 2 represent the result of the latter procedure (with

indices i and j running from 0 to 4) applied to $0.5m$ Na_2SO_4 at pressures up to 0.03 GPa and temperatures to 300°C. The specific volume is then

$$v_{sp} = \left(\frac{\partial G_{sp}}{\partial P}\right)_T \tag{4}$$

If f is the fraction, by weight, of solute in a binary mixture, the quantity $v_{sp}/(1-f)$ is the volume of the solution that contains 1 g of solvent. The number of moles (n) of a solute species with formula weight w in this volume is then $n = f/(1-f)\,w$. It is convenient to introduce the definition $y = v_{sp}/(1-f) - v^\circ$, where v° is the specific volume of the pure solvent.

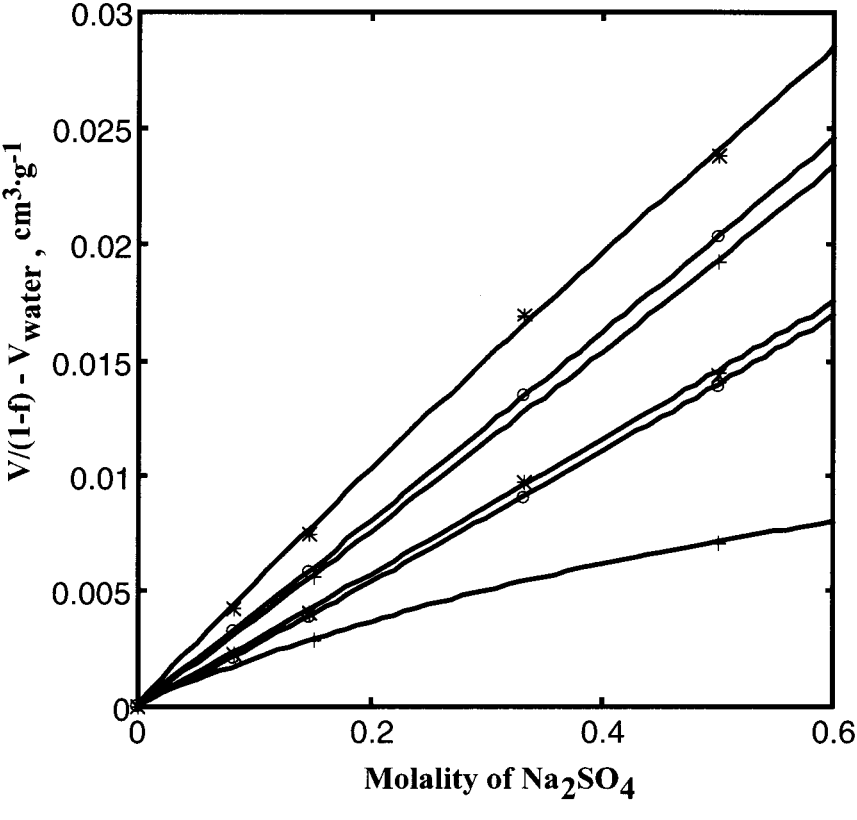

Fig. 4. Effect of temperature and pressure on the specific volume of aqueous sodium sulfate at higher pressures. The quantity y at 0.1 GPa (lower three curves) and 0.5 GPa (upper three curves) is plotted versus molality at 25°C (∗), 100°C (○), and 200°C (+).

Differentiation of y with respect to n gives the partial molal volume of the solute, $\bar{V}$. Integration of the expression,

$$\left(\frac{\partial \mu}{\partial P}\right)_{TP} = \bar{V} \tag{5}$$

then yields the pressure dependence of μ, the chemical potential of the solute species at any composition. A representative plot of y *versus* n is given in Fig. 4, where the initial slope determines the pressure derivative of the standard chemical potential, and the deviation from linearity the pressure dependence of the excess free energy.

3. THERMAL DIFFUSIVITY

When the acoustic disturbance has been fully damped, a spatially periodic distribution of temperature and, hence, index of refraction, remains. This grating decays exponentially by thermal diffusion with a characteristic

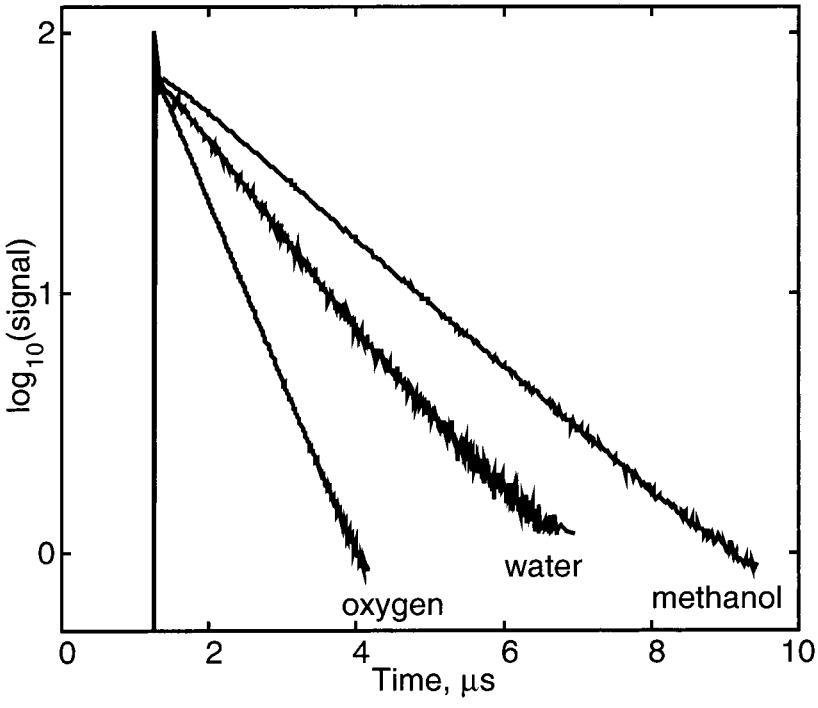

Fig. 5. Semilogarithmic plots of the Bragg-scattered intensity from oxygen in the diamond-anvil cell (12.7 GPa, 300°C), as well as from water and methanol under ambient conditions.

time, τ, given by $\tau^{-1} = 4\pi^2 D d^{-2}$, where D is the thermal diffusivity (the thermal conductivity divided by the heat capacity per unit volume) of the fluid. The variation of τ with d serves to distinguish thermal diffusion from other relaxation processes and, at high temperatures, permits a straightforward separation of nondiffusive radiative transport from diffusive processes. Given the long thermal relaxation times characteristic of molecular fluids, in the case of a strong signal, a continuous (argon ion) laser may be substituted for the pulsed probe and the signal can be captured with a transient recorder over the full duration of the decay, for each pulse of the excitation laser. Semilog plots of such data are given in Fig. 5 for oxygen in the diamond-anvil cell at 300°C and 12.7 GPa, as well as for water and methanol under ambient conditions.

4. DISCUSSION

Sodium sulfate was selected for preliminary studies both as a representative and relatively nonreactive electrolyte and as a proposed major constituent of "Europa's briny deep" [12]. The determination of the specific volume at higher pressures by integration of Eq. (2) is based, up to 150°C, on experimental values at ambient pressure or along the coexistence curve

Table II. Specific Volume ($cm^3 \cdot g^{-1}$) of 0.5 and 0.148m Aqueous Na_2SO_4 as a Function of Temperature and Pressure

	0.500m				0.148m			
P (MPa)	25°C	100°C	130°C	200°C	25°C	100°C	130°C	200°C
0.10	0.9454	0.9832			0.9844	1.0240		
27.0	0.9358	0.9723	0.9934	1.0573	0.9734	1.0117	1.0345	1.1110
100	0.9131	0.9468	0.9652	1.0175	0.9476	0.9833	1.0026	1.0628
200	0.8876	0.9188	0.9348	0.9774	0.9189	0.9532	0.9687	1.0165
400	0.8494	0.8764	0.8901	0.9227	0.8766	0.9064	0.9195	0.9554
600	0.8213	0.8448	0.8571	0.8850			0.8834	0.9135
800		0.8198	0.8311	0.8559			0.8560	0.8819
1000			0.8096	0.8320			0.8332	0.8564
1200		0.7819	0.7913	0.8119			0.8141	0.8349
1400		0.7667	0.7753	0.7946			0.7977	0.8165
1600		0.7533	0.7612	0.7793			0.7832	0.8004
1800			0.7485	0.7656			0.7704	0.7861
2000			0.7371	0.7533			0.7589	0.7733
2400			0.7173	0.7315			0.7388	0.7510
2800			0.7005	0.7129			0.7217	0.7322
3400				0.6896				0.7085

[13, 14]. The specific volume as a function of pressure; temperature, and concentration is given in Table II.

The acoustic velocities that are the principal determinants of the change in density with respect to pressure are measured to 0.2%. It is likely that below 150°C, the errors in the specific volumes in Table II are not much larger than the errors in the initial densities, in particular, in the values at temperatures above 100°C along the coexistence curve. At the higher pressures explored in the diamond-anvil cell, the pressure derivative of the speed of sound is roughly $1000\,m \cdot s^{-1} \cdot GPa^{-1}$. Random errors in speed of sound of approximately $\pm 30\,m \cdot s^{-1}$, consequent upon errors in the measurement of pressure, must be expected. This is consistent with the departures from smooth variation of the speed of sound with temperature and pressure as exhibited by the data in Table I. A systematic error of 0.1% in the speed of sound would contribute an error of $\approx 0.08\%$ in the specific volume at 3.5 GPa and an error of $\approx 2\,cm^3 \cdot mol^{-1}$ in the apparent partial molal volume in a 0.5 molal solution.

The partial molar volume of Na_2SO_4 at infinite dilution is given as a function of temperature and pressure in Table III. At high temperatures and low pressures, the large negative electrostrictive contribution predominates. Indeed, below 0.03 GPa the pressure and temperature dependence of V° can be calculated from the temperature and pressure dependence of the dielectric constant of water [15]. The increase in V° with P at pressures above 0.1 GPa cannot, however, be interpreted as being due principally to a decrease in the magnitude of the negative electrostrictive term.

The thermal diffusivities of fluid oxygen have been measured to pressures higher than 12 GPa and at temperatures from 25 to 300°C;

Table III. Partial Molal Volumes ($cm^3 \cdot mol^{-1}$) of Na_2SO_4 at Infinite Dilution as a Function of Temperature and Pressure

	P (MPa)										
T (°C)	0.100	6.8	16.0	27.0	100	200	300	500	800	1600	2400
25	12.1	13.8	15.2	16.6	24.7	33.0	40.4	50.5			
50	13.4	14.5	15.7	16.8	24.9	31.2	36.4	44.3	52.9		
100	10.3	11.4	12.8	14.2	21.9	27.0	31.0	37.3	44.7	58.9	
130		1.3	2.9	4.5	15.0	23.8	30.4	38.4	49.4		
150		−6.3	−4.2	−1.5							
190		−34.6	−30.3	−25.5							
200		−41.8	−36.2	−30.9	11.6	22.4	27.6	33.8	37.8	46.1	59.0
230		−79.2	−69.5	−59.8							
250		−120	−104	−89.1							

results are discussed in Ref. 16. Typically, measurements have been made with the use of a continuous probe laser to an accuracy of 2%. Oxygen provides a particularly large signal due to a resonant electronic transition at the fundamental frequency of our Nd:YAG laser. At elevated pressures most other materials, in particular, water, yield smaller signals, which necessitates the use of a pulsed probe; the accuracy of the results should be comparable.

ACKNOWLEDGMENTS

This work was supported by Grants EAR 96-14313 and EAR 98-14599 from the National Science Foundation and by research subcontract B5030002 from the Lawrence Livermore National Laboratory.

REFERENCES

1. T. J. Ahrens, *Nature* **342**:122 (1989); J. M. Delaney and H. C. Helgeson, *Am. J. Sci.* **278**:638 (1978).
2. D. J. Stevenson and E. E. Salpeter, *Astrophys. J. Suppl.* **35**:221 (1977).
3. A. W. Lawson, E. Lowell, and A. L. Jain, *J. Chem. Phys.* **30**:643 (1959).
4. B. Le Neindre, Y. Garrabos, and R. Tufa, *Physica A* **152**:512 (1989).
5. M. D. Fayer, *Annu. Rev. Phys. Chem.* **33**:63 (1987).
6. Y. X. Yan, L. T. Cheng, and K. A. Nelson, in *Advances in Nonlinear Spectroscopy*, J. H. Clark and R. E. Hester, eds. (Wiley, London, 1987).
7. J. Zaug, L. U. Slutsky, and J. M. Brown, *J. Phys. Chem.* **98**:6008 (1994).
8. J. Zaug, E. H. Abramson, J. M. Brown, and L. J. Slutsky, in *High Pressure Research; Applications to Earth and Planetary Sciences*, Y. Syono and M. Manghnani, eds. (American Geophysical Union, Washington, DC, 1992), p. 157.
9. H. K. Mao, P. M. Bell, J. W. Shaner, and D. J. Steinberg, *J. Appl. Phys.* **49**:3276 (1978).
10. G. J. Piermarini, S. Block, and J. D. Barnett, *J. Appl. Phys.* **44**:5377 (1973).
11. S. C. Schmidt, D. Shiferl, A. S. Zinn, D. D. Ragan, and D. S. Moore, *J. Appl. Phys.* **69**:2793 (1991).
12. J. S. Kargel, *Icarus* **94**:368–390 (1991); *Science* **280**:1211 (1998).
13. P. S. Z. Rogers and K. S. Pitzer, *J. Phys. Chem.* **85**:2886 (1981).
14. A. Korosi and B. M. Fabuss, *J. Chem Eng. Data* **13**:548 (1968); C. D. Synowietz, J. Dans, and H. Surawski, *Densities of Binary Aqueous Systems and Heat Capacities of Liquid Systems. IV (Macroscopic and Technical Properties of Matter.). Numerical Data and Functional Relationships in Science and Technology*, Landolt Bornstein, Zahlenwerte and Funktionen, Band II, Teil 1 (Springer, Berlin, 1971).
15. E. H. Abramson, J. M. Brown, and L. J. Slutsky, *Ann. Rev. Phys. Chem.* **50**:279 (1999).
16. E. H. Abramson, L. J. Slutsky, and J. M. Brown, *J. Chem. Phys.* **111**:9357 (1999).